UTI
Urogenital Tract Infection

Original Article

pISSN 2465-8243 • eISSN 2465-8510
Urogenit Tract Infect 2026;21(1):26-39
https://doi.org/10.14777/uti.2550046023

Identification of Plasma Biomarker Signatures for Acute and Chronic Cystitis Using Olink Explore Proteomics in UK Biobank

Chang Gu Kang, Su Kang Kim

Department of Biomedical Laboratory Science, Catholic Kwandong University, Gangneung, Korea

Received December 3, 2025
Revised February 2, 2026
Accepted February 14, 2026

Corresponding author:
Su Kang Kim
Department of Biomedical Laboratory Science, Catholic Kwandong University, 24, Beomil-ro 579beon-gil, Gangneung 25601, Korea
Email: skkim7@cku.ac.kr
https://orcid.org/0000-0001-6178-8514

Purpose: Acute and chronic cystitis represent common yet biologically distinct inflammatory disorders of the lower urinary tract. However, circulating biomarkers capable of differentiating these conditions remain poorly defined.

Materials and Methods: Using COMPASS-processed Olink Explore proteomic data from UK Biobank participants, we compared plasma protein profiles across individuals with acute cystitis, chronic cystitis, and normal controls. After stringent quality-control procedures, covariate-adjusted regression models and differential abundance analyses were performed. STRING-based protein-protein interaction (PPI) networks were constructed to examine systems-level organization of significantly altered proteins.

Results: Among 2,715 participants, acute and chronic cystitis demonstrated distinct systemic proteomic signatures. CHGA (chromogranin A) and GAST (gastrin) were consistently elevated across both phenotypes, indicating shared neuroendocrine-associated systemic responses. Acute cystitis showed selective elevation of CDH2 (cadherin-2), whereas chronic cystitis demonstrated marked increases in GDF15 (growth differentiation factor 15). PPI network analysis revealed a densely interconnected architecture in acute cystitis and a more modular, branch topology in chronic cystitis, reflecting differing organizational patterns of circulating proteins.

Conclusions: This population-level analysis identifies phenotype-specific and shared plasma protein signatures associated with acute and chronic cystitis and provides an initial framework for understanding systemic inflammatory profiles in these conditions. Interpretation should remain cautious given the cross-sectional design, reliance on historical diagnostic classification, and the absence of bladder-specific molecular data. Nonetheless, these findings highlight candidate biomarkers that merit further validation in longitudinal and mechanistic studies.

Keywords: Acute cystitis, Chronic cystitis, Biomarkers, Proteomics, UK Biobank

• **Funding/Support:** This research was supported by the Regional Innovation System & Education (RISE) program through the Gangwon RISE Center, funded by the Ministry of Education (MOE) and the Gangwon State (G.S.), Republic of Korea (2025-RISE-10-001).
• **Research Ethics:** Ethical review and approval were waived by the institutional review board (IRB) of Kangwon National University (IRB No. 2025-05-014) because this study involved secondary analysis of fully deidentified UK Biobank data (application number: 52031).
• **Conflict of Interest:** The authors have nothing to disclose.

HIGHLIGHTS

Population-scale Olink proteomic profiling in the UK Biobank identified both shared and phenotype-specific plasma signatures in acute and chronic cystitis. CHGA (chromogranin A) and GAST (gastrin) were consistently elevated across both conditions, whereas CDH2 (cadherin-2) and GDF15 (growth differentiation factor 15) exhibited phenotype-specific increases in acute and chronic cystitis, respectively. Protein-protein interaction network analysis revealed distinct organizational patterns, with dense connectivity in acute disease and a more modular architecture in chronic cystitis.

INTRODUCTION

Cystitis is a highly prevalent bladder-specific inflammatory disorder that poses a substantial clinical burden, particularly among women [1]. Acute cystitis most commonly results from short-term bacterial infection or a transient inflammatory insult and presents with dysuria, urgency, and suprapubic discomfort [2]. In contrast, chronic cystitis involves persistent or recurrent urothelial inflammation, often associated with repeated episodes of infection or ongoing mucosal injury, and is characterized by long-standing symptoms that necessitate ongoing clinical evaluation and management [3]. Although acute and chronic forms display distinct clinical trajectories, their underlying biological mechanisms remain poorly defined. Clinicians still primarily rely on symptoms, urinalysis, and culture findings, which offer limited insight into systemic inflammatory activity or the transition from acute to chronic disease. Consequently, reliably distinguishing patients with early acute inflammation from those with evolving chronic pathology remains difficult, underscoring the need for improved molecular or proteomic markers.

Growing evidence indicates that cystitis involves intricate interactions among urothelial barrier function [4], neuroimmune signaling [5], and systemic inflammatory mediators [6]. Acute inflammation is characterized by rapid activation of innate immune pathways, including epithelial antimicrobial responses and early cytokine release [7]. In contrast, chronic inflammation is associated with sustained cytokine and chemokine signaling [8] and epithelial remodeling [9]. However, the molecular signatures that reliably distinguish acute from chronic disease remain poorly defined in human populations. Most available insights are derived from animal models or localized bladder tissue analyses, and few studies have investigated circulating biomarkers that could enable minimally invasive diagnosis or reflect systemic inflammatory activity.

Advances in high-throughput proteomic profiling now allow large-scale characterization of circulating proteins in population-based cohorts. The UK Biobank recently incorporated Olink Explore proteomic measurements, which use proximity extension assays to quantify a broad panel of plasma proteins with high sensitivity. When paired with detailed phenotype data, these proteomic profiles enable systematic assessment of inflammatory, epithelial, and immune-related pathways across diverse clinical conditions [10,11].

In this study, we aimed to identify circulating plasma protein signatures that distinguish acute cystitis from chronic cystitis in a large population-based cohort. Using UK Biobank proteomic data, our primary objective was to characterize phenotype-specific and shared systemic protein profiles associated with these two clinically distinct forms of cystitis, and to explore their potential relevance as candidate biomarkers for disease stratification and biological characterization.

MATERIALS AND METHODS

1. Cohort Definition and Covariates

Ethical review and approval were waived by the institutional review board (IRB) of Kangwon National University (IRB No. 2025-05-014) because this study involved secondary analysis of fully deidentified UK Biobank data (application number: 52031). Participants were classified into acute cystitis, chronic cystitis, and normal control groups using diagnosis-based phenotype data curated through the COMPASS platform. Acute cystitis (International Classification of Diseases, Tenth Revision [ICD-10] code N30.0) and chronic cystitis (ICD-10 codes N30.1 and N30.2) were defined based on clinically recorded diagnoses from linked hospital inpatient and primary care datasets. Normal controls were defined as individuals without any recorded diagnosis of cystitis (ICD-10 code N30). Cases classified as other cystitis (ICD-10 code N30.8) or unspecified cystitis (ICD-10 code N30.9) were excluded to reduce phenotypic heterogeneity. To construct a relatively healthy reference group, individuals with major cardiometabolic conditions, including hypertension, diabetes, or dyslipidemia, were excluded. The

diagnoses were based on historical medical records and may not necessarily reflect active disease status at the time of blood sampling.

2. UK Biobank Cohort and COMPASS Platform–Based Data Extraction

Plasma proteomic catalogued under UK Biobank data-field 30900 and clinical data were obtained from the UK Biobank under approved access. Participants with Olink Explore proteomics measurements were identified using the COMPASS platform (Cipherome Inc., USA), which provides preprocessed Olink NPX matrices and harmonized metadata for UK Biobank participants. Within COMPASS, we restricted the dataset to individuals with available Olink Explore proteomics data. Proteomic measurements were derived from baseline assessment blood samples collected during the initial UK Biobank recruitment period (2006–2010).

3. Quality Control of Olink Proteomics and Metadata

Plasma proteomic measurements generated using the Olink Explore platform were obtained from the UK Biobank and processed with the COMPASS normalization pipeline (Cipherome Inc.), which provides $\log_2$-scaled normalized protein expression (NPX) values and detailed assay metadata. Participant demographics, clinical phenotype information, sample collection dates, and Olink proteomics metadata (including batch, plate, and assay identifiers) were merged using unique participant and sample identifiers. Assay-specific limits of detection (LOD) were incorporated by mapping the first token of each protein name to its corresponding assay-level LOD value. Protein values falling below the assay LOD were flagged, and proteins with more than 25% of samples below the LOD were removed. Likewise, samples with more than 10% of protein measurements below the LOD were excluded. After LOD filtering, missingness was assessed across the remaining dataset, and proteins or samples with more than 20% missing values were removed. Technical variation associated with the sample collection date was evaluated by computing date-specific mean NPX values and identifying date outliers using a z-score threshold of $|Z| > 3$. Samples collected on outlier dates were excluded. Sample collection dates were then converted into numeric form as the number of days since the earliest collection, enabling covariate adjustment for temporal drift in downstream modeling. After these quality-control steps, a cleaned expression matrix and harmonized metadata table were generated for subsequent analysis.

4. Statistical Modeling and Differential Protein Analysis

Protein NPX values were modeled using ordinary least-squares linear regression, implemented in Python using the statsmodels package. For each protein, NPX values were modeled as a function of disease status, with age, sex, and sample collection date included as covariates. Proteins with insufficient nonmissing values within either group were excluded prior to analysis.

For each comparison, effect sizes (case minus control), raw p-values, and Benjamini-Hochberg false discovery rate (FDR)–adjusted q-values were calculated. Proteins with $q<0.05$ were considered statistically significant. FDR correction was applied across all tested proteins using the Benjamini-Hochberg method.

Visualization included volcano plots, displaying effect size on the *x*-axis and $-\log_{10}$(p-value) on the *y*-axis, with FDR-significant proteins highlighted and the top 10 most significant proteins annotated. Heatmaps were generated based on mean NPX values of top differentially abundant proteins, using a diverging color palette to illustrate relative expression differences between groups.

All analyses and figure generation were performed in Python (v3.8) using pandas, numpy, statsmodels, matplotlib, and adjustText, within a fully reproducible workflow integrating data preprocessing, quality control, differential modeling, and visualization.

Table 1. Baseline demographic and clinical characteristics of the study population

Variable	Normal (n=2,295)	Acute cystitis (n=260)	Chronic cystitis (n=160)
Age (yr)	68.8±7.8	73.8±7.8	75.6±7.0
Sex			
Female	1,180 (51.4)	235 (90.4)	88 (55.0)
Male	1,115 (48.6)	25 (9.6)	72 (45.0)
Diabetes mellitus			
No	2,295 (100)	235 (90.4)	133 (83.1)
Yes	-	25 (9.6)	27 (16.9)
Hypertension			
No	2,295 (100)	153 (58.8)	60 (37.5)
Yes	-	107 (41.2)	100 (62.5)
Hyperlipidemia			
No	2,295 (100)	237 (91.2)	145 (90.6)
Yes	-	23 (8.8)	15 (9.4)

Values are presented as mean±standard deviation or number (%).
Diabetes mellitus, hypertension, and hyperlipidemia were defined based on the corresponding binary variables in the dataset (yes/no).
Normal, acute cystitis, and chronic cystitis groups were defined according to the clinical classification in the study cohort.

RESULTS

1. Demographic Characteristics Across Acute, Chronic, and Normal Groups

From the approximately 500,000 participants in the UK Biobank cohort, 53,039 individuals with available Olink Explore plasma proteomic data were initially identified. Among these participants, normal controls were defined as individuals with no recorded medical diagnoses across hospital inpatient records, primary care data, or self-reported health records. Acute and chronic cystitis cases were identified based on diagnosis histories indicating acute or chronic cystitis, respectively, as curated within the COMPASS platform. After applying phenotype-based classification and proteomic quality-control procedures, the final analytical sample consisted of 2,715 participants, including 2,295 normal controls, 260 individuals with acute cystitis, and 160 individuals with chronic cystitis.

A total of 2,715 participants were included in the analysis, consisting of 2,295 normal controls, 260 individuals with acute cystitis, and 160 individuals with chronic cystitis. The cystitis groups were markedly older than normal controls, with mean ages of 73.8±7.8 years in the acute group and 75.6±7.0 years in the chronic group, compared with 68.8±7.8 years among controls. As expected, given the epidemiology of urinary tract infections, the acute cystitis group demonstrated a strong female predominance (235 women, 25 men; 90.4% female). In contrast, the chronic cystitis group showed a more balanced sex distribution (88 women, 72 men; 55.0% female), while the normal group exhibited near-equal representation of women and men (1,180 women, 1,115 men; 51.4% female) (Table 1). Age and sex were therefore incorporated as covariates in all subsequent statistical analyses to minimize demographic confounding.

2. Differential Plasma Protein Signatures in Acute Cystitis

Before quality control, the study included 2,295 normal controls and 260 individuals with acute cystitis.

After applying the proteomics quality-control procedures (LOD-based filtering, missingness filtering, and date outlier removal), 1,921 normal controls and 217 individuals with acute cystitis were retained for the final analysis.

In the comparison between normal controls and individuals with acute cystitis, several plasma proteins showed statistically significant differential abundance af-

ter adjustment for age, sex, and sample collection date. Multiple proteins passed the FDR threshold of q〈0.05, indicating robust differences between groups. A summary of the top differentially abundant proteins is summarized in Table 2 and illustrated in Figs. 1 and 2.

The most significantly altered protein was chromogranin A (CHGA), which exhibited markedly higher NPX levels in the acute cystitis group compared with the normal group (effect size=0.3541, FDR=7.996×10^{-9}). CHGA is a neuroendocrine-derived secretory protein implicated in inflammatory and stress-response pathways, suggesting its potential involvement in neuroimmune mechanisms underlying cystitis.

The second most significant protein was cadherin-2 (CDH2), a calcium-dependent adhesion molecule known to promote epithelial-mesenchymal transition and tissue remodeling, may reflect systemic responses associated with inflammatory or epithelial injury processes. CDH2 levels were significantly elevated in acute cystitis (effect size=0.1742, FDR=3.760×10^{-6}).

Additionally, gastrin (GAST) showed substantial upregulation (effect size=0.4643, FDR=1.305×10^{-5}). Although GAST is classically known for its role in gastric acid secretion, emerging evidence supports its immunomodulatory roles, suggesting that elevated circulating GAST may reflect systemic inflammatory activation secondary to acute urinary tract inflammation.

These protein-level differences are visually summarized in Fig. 1, which depicts both the overall differential expression landscape and the magnitude of group-wise expression differences.

Fig. 1A shows a volcano plot illustrating effect sizes (case versus normal) versus statistical significance, highlighting FDR-significant proteins in red and labeling the most strongly altered markers (CHGA, CDH2, and GAST). Fig. 1B presents a heatmap of the top 20 differentially abundant proteins, displaying mean NPX values for each group and revealing a clear pattern of upregulated inflammatory and epithelial-response proteins in acute cystitis.

Together, CHGA, CDH2, and GAST represent the top differentially abundant plasma proteins distinguishing acute cystitis from normal individuals, collectively implicating pathways related to neuroendocrine activation, epithelial remodeling, cytokine regulation, and systemic inflammatory response. The integrated evidence from both quantitative analysis (Table 2) and visual summaries (Fig. 1) underscores a distinct plasma proteomic profile associated with acute cystitis.

3. Differential Plasma Protein Signatures in Chronic Cystitis

Before quality control, the study included 2,295 normal controls and 160 individuals with chronic cystitis.

After applying the proteomics quality-control procedures (LOD-based filtering, missingness filtering, and date outlier removal), 1,921 normal controls and 127 individuals with chronic cystitis were retained for the final analysis.

In the comparison between normal controls and individuals with chronic cystitis, we identified a strong and consistent pattern of upregulated circulating proteins associated with immune activation, epithelial injury, and chronic inflammatory remodeling (Table 3; Figs. 3 and 4). Among all detected proteins, CHGA showed the greatest elevation in chronic cystitis, increasing from -0.070 NPX in controls to 0.494 NPX in patients (effect=0.474; FDR=2.02×10^{-10}).

The second most significantly elevated protein was GAST, which exhibited a marked increase from 0.061 to 0.906 NPX (effect=0.737; FDR=1.53×10^{-9}). Growth differentiation factor 15 (GDF15) also demonstrated a substantial elevation (effect=0.232; FDR=9.99×10^{-8}).

In Fig. 3A, the volcano plot highlights significantly altered proteins (FDR 〈 0.05 in red), with CHGA, GAST, and GDF15 showing the strongest effect sizes. Fig. 3B presents a heatmap of the top 20 most significant proteins, illustrating their mean NPX levels in each group and demonstrating clear separation between chronic cystitis and normal controls.

Table 2. Top differentially abundant proteins between normal controls and acute cystitis

Symbol	Normal (mean)	Acute cystitis (mean)	Effect	p-value	Normal (n)	Acute cystitis (n)	FDR	95% CI	Missing data (n)	
									Normal	Acute cystitis
CHGA	-0.07	0.345	0.3541	3.72E-12	1,901	216	8.00E-09	0.255–0.453	394	44
CDH2	-0.103	0.069	0.1742	3.50E-09	1,888	211	3.76E-06	0.117–0.232	407	49
GAST	0.061	0.661	0.4643	1.82E-08	1,904	213	1.31E-05	0.303–0.625	391	47
IL18BP	-0.081	0.051	0.1113	1.82E-06	1,886	211	0.001	0.066–0.157	409	49
HLA	-0.057	0.066	0.1038	2.03E-06	1,884	211	0.001	0.061–0.147	411	49
GDF15	-0.186	0.065	0.1347	2.38E-06	1,895	216	0.001	0.079–0.191	400	44
IGFBP4	-0.144	0.065	0.1423	2.71E-06	1,857	213	0.001	0.083–0.202	438	47
REN	-0.06	0.039	0.2395	2.89E-06	1,888	211	0.001	0.139–0.340	407	49
CRYBB2	0.081	0.32	0.1987	1.21E-05	1,904	213	0.003	0.110–0.288	391	47
DNER	0.084	-0.062	-0.0984	1.68E-05	1,886	212	0.003	-0.143 to -0.054	409	48
SHISA5	-0.076	0.033	0.0756	1.92E-05	1,901	216	0.003	0.041–0.110	394	44
TNFRSF1B	-0.083	0.048	0.1076	2.09E-05	1,883	214	0.003	0.058–0.157	412	46
ASGR1	-0.085	0.012	0.1062	2.10E-05	1,897	213	0.003	0.057–0.155	398	47
PIGR	-0.076	0.07	0.1219	3.05E-05	1,860	213	0.005	0.065–0.179	435	47
CELA2A	0.01	-0.11	-0.1855	3.40E-05	1,901	216	0.005	-0.273 to -0.098	394	44
ADM	-0.155	0.018	0.1009	4.28E-05	1,906	215	0.006	0.053–0.149	389	45
TFPI2	-0.04	0.194	0.1284	6.28E-05	1,893	215	0.008	0.066–0.191	402	45
CXCL9	-0.126	0.222	0.1996	7.66E-05	1,894	214	0.009	0.101–0.298	401	46

Values are presented as mean covariate-adjusted normalized protein expression values and regression effect estimates (acute cystitis vs. normal controls).
Although the total numbers of participants classified as normal controls and acute cystitis were 2,295 and 260, respectively, the numbers of samples used for each protein (n_normal and n_acute cystitis) vary because proteins and samples failing predefined quality-control criteria (including limits of detection and missingness thresholds) were excluded on a per-protein basis.
FDR, false discovery rate; CI, confidence interval.

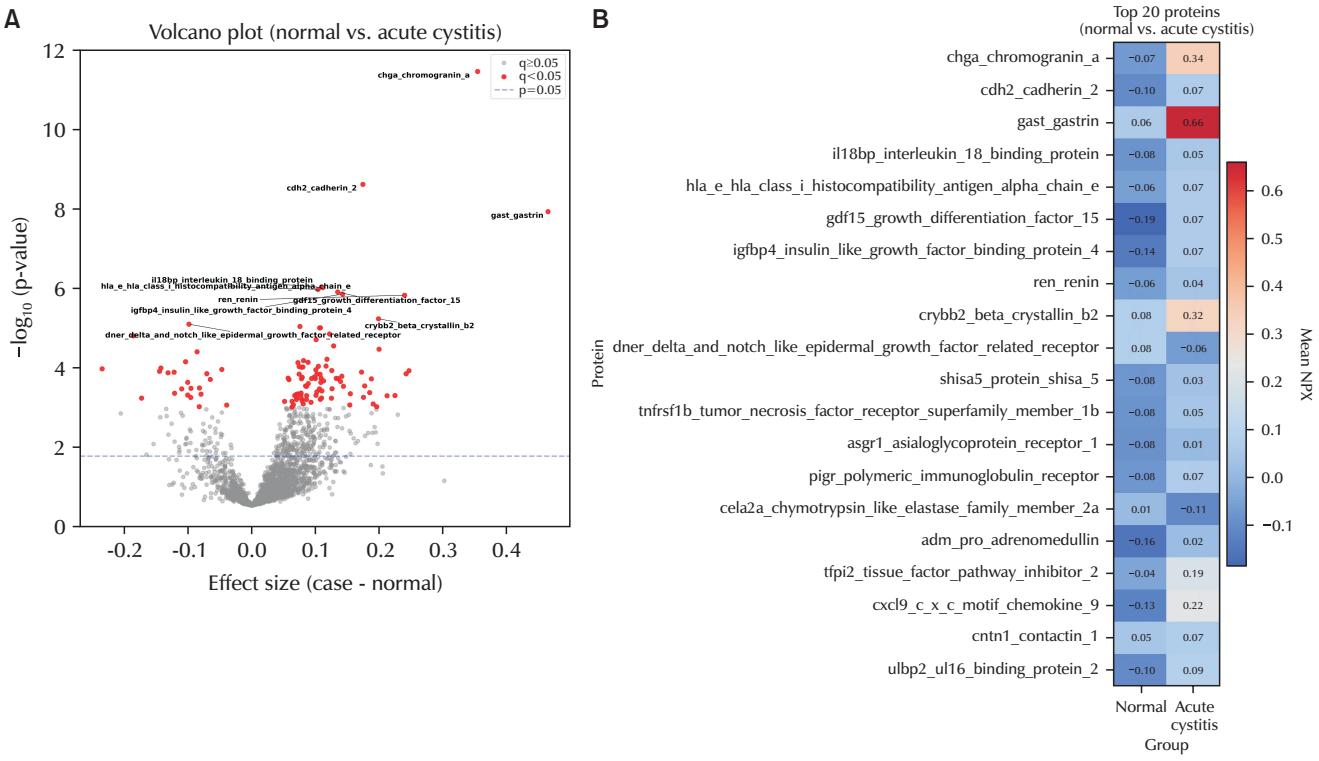

Fig. 1. Differential expression landscape and top protein signatures in acute cystitis. (A) Volcano plot illustrating the distribution of differential plasma proteins between acute cystitis and normal individuals. Significantly altered proteins (FDR<0.05) are shown in red, and the top markers (*CHGA*, *GAST*, *CDH2*) are labeled. These proteins exhibit strong effect sizes and highly significant p-values, indicating robust proteomic shifts during acute inflammation. (B) Heatmap of the top 20 most significant proteins ranked by p-value, showing mean NPX expression in each group. Acute cystitis displays distinct upregulation of neuroendocrine markers (*CHGA*), epithelial stress markers (*CDH2*), and inflammatory mediators (*IL18BP*, *TNFRSF1B*), forming a clear disease-associated proteomic signature. FDR, false discovery rate; NPX, normalized protein expression.

4. PPI Network Analysis of Differentially Abundant Proteins

To further contextualize the differentially abundant proteins, STRING-based PPI networks were constructed separately for acute and chronic cystitis (Fig. 5). The resulting networks displayed distinct organizational architectures.

In acute cystitis, the PPI network formed a densely interconnected configuration, characterized by numerous high-degree nodes and tightly clustered ligand-receptor groupings (Fig. 5A). Prominent interaction hubs included tumor necrosis factor (TNF), TNF receptor superfamily member 1A/B (TNFRSF1A/B), ICAM1 (intercellular adhesion molecule 1), CD80, and CD83, accompanied by compact submodules involving TNFRSF10A/B, CD27-associated proteins, and fibroblast growth factor-related interactions. The overall architecture reflects a highly integrated interaction framework with extensive cross-linking among multiple protein clusters (Fig. 5A).

In contrast, the chronic cystitis network exhibited a more linear and spatially dispersed topology with fewer, yet clearly delineated, interaction branches (Fig. 5B). Central nodes, including CHGA, GAST, GDF15, and TNFRSF1B, anchored the network, which extended into peripheral branches containing proteins such as CXCL9 (chemokine [C-X-C motif] ligand 9), IL18BP (interleukin-18 binding protein), ADM (adrenomedullin), REN (renin), PILRA (paired immunoglobin-like type 2 receptor alpha), and ASGR1 (asialoglycoprotein receptor 1). Compared with the acute network, the chronic network demonstrated reduced connectivity and a more directional, branch-like structural arrangement (Fig. 5B).

Together, these PPI networks underscore substantial architectural differences between acute and chronic

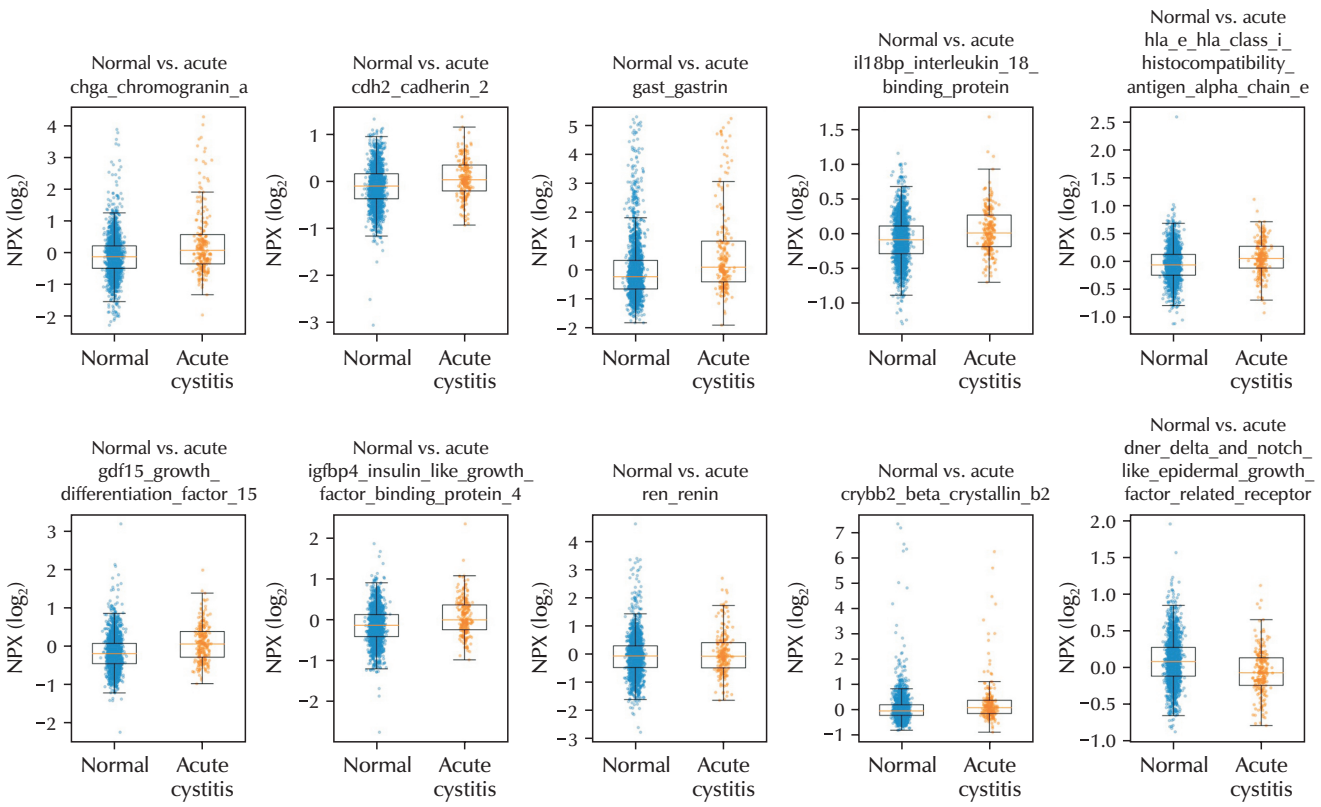

Fig. 2. Box plots of normalized protein expression (NPX) (log_2) values for the top proteins significantly altered in acute cystitis compared with normal controls. Blue denotes normal controls and orange denotes acute cystitis. Individual data points are overlaid, showing consistent upregulation of markers such as *CHGA*, *CDH2*, and *GAST* in acute cystitis.

cystitis, with the acute network displaying a compact, highly interconnected configuration and the chronic network exhibiting a streamlined, modular organization. These structural distinctions complement the differential abundance findings and support the presence of distinct proteomic patterns across the two disease states.

DISCUSSION

The UK Biobank recently incorporated Olink Explore proteomic measurements for nearly 50,000 participants, enabling large-scale case–control analyses across a broad spectrum of diseases. Multiple recent studies have used this resource to characterize circulating protein signatures associated with cardiovascular, metabolic, and inflammatory conditions. Within this expanding landscape of population-scale proteomics, our study examined whether acute and chronic cystitis exhibit distinguishable plasma biomarker profiles. We identified distinct protein signatures separating the 2 groups, indicating measurable systemic differences between acute and chronic cystitis within this cross-sectional dataset.

In this population-scale proteomic analysis, we identified distinct plasma signatures that differentiate acute cystitis from chronic cystitis. Across both acute and chronic cystitis, CHGA and GAST emerged as the most consistently elevated proteins. Previous studies have described CHGA as a circulating marker associated with neuroendocrine activation and systemic stress responses [12-15], while GAST has been reported to participate in broader inflammatory or regulatory signaling in non-gastrointestinal contexts [16]. Although the present cross-sectional design does not allow mechanistic inference, the consistent elevation of these proteins in both acute and chronic cystitis suggests that they represent

Table 3. Top differentially abundant proteins between normal controls and chronic cystitis

Symbol	Normal (mean)	Chronic cystitis (mean)	Effect	p-value	Normal (n)	Chronic cystitis (n)	FDR	95% CI	Missing data (n)	
									Normal	Chronic cystitis
CHGA	-0.07	0.494	0.474	9.38E-14	1,901	125	2.02E-10	0.350–0.598	394	35
GAST	0.061	0.906	0.737	1.42E-12	1,904	127	1.53E-09	0.534–0.939	391	33
GDF15	-0.186	0.224	0.232	1.39E-10	1,895	127	9.99E-08	0.162–0.303	400	33
PLAUR	-0.088	0.13	0.165	1.39E-09	1,878	123	7.45E-07	0.112–0.219	417	37
TNFRSF1A	-0.082	0.139	0.165	4.23E-09	1,883	127	1.82E-06	0.110–0.220	412	33
IGFBP4	-0.144	0.183	0.224	1.16E-08	1,857	127	4.17E-06	0.147–0.301	438	33
HAVCR1	-0.242	0.323	0.341	1.43E-08	1,905	126	4.40E-06	0.224–0.459	390	34
HAVCR2	-0.108	0.141	0.187	3.73E-08	1,883	127	1.00E-05	0.120–0.253	412	33
WFDC2	-0.103	0.2	0.19	6.25E-08	1,795	122	1.49E-05	0.121–0.258	500	38
VSIG2	-0.079	0.268	0.249	1.24E-07	1,896	126	2.65E-05	0.157–0.340	399	34
TNFRSF1B	-0.083	0.131	0.168	1.35E-07	1,883	127	2.65E-05	0.106–0.230	412	33
PILRA	-0.149	0.146	0.218	1.59E-07	1,883	127	2.80E-05	0.137–0.300	412	33
TREM2	-0.199	0.226	0.268	1.69E-07	1,883	124	2.80E-05	0.168–0.368	412	36
LGALS9	-0.114	0.133	0.162	5.21E-07	1,889	125	8.01E-05	0.099–0.225	406	35
FSTL3	-0.103	0.144	0.158	6.56E-07	1,880	123	9.00E-05	0.096–0.220	415	37
RAB6A	0.078	-0.13	-0.237	6.70E-07	1,884	125	9.00E-05	-0.33 to -0.144	411	35

Values are presented as mean covariate-adjusted normalized protein expression values and regression effect estimates (chronic cystitis vs. normal controls). Although the total numbers of participants classified as normal controls and chronic cystitis were 2,295 and 160, respectively, the numbers of samples used for each protein (n_normal and n_chronic cystitis) differ across proteins because measurements failing predefined quality-control criteria (including limits of detection and missingness thresholds) were excluded on a per-protein basis.
FDR, false discovery rate; CI, confidence interval.

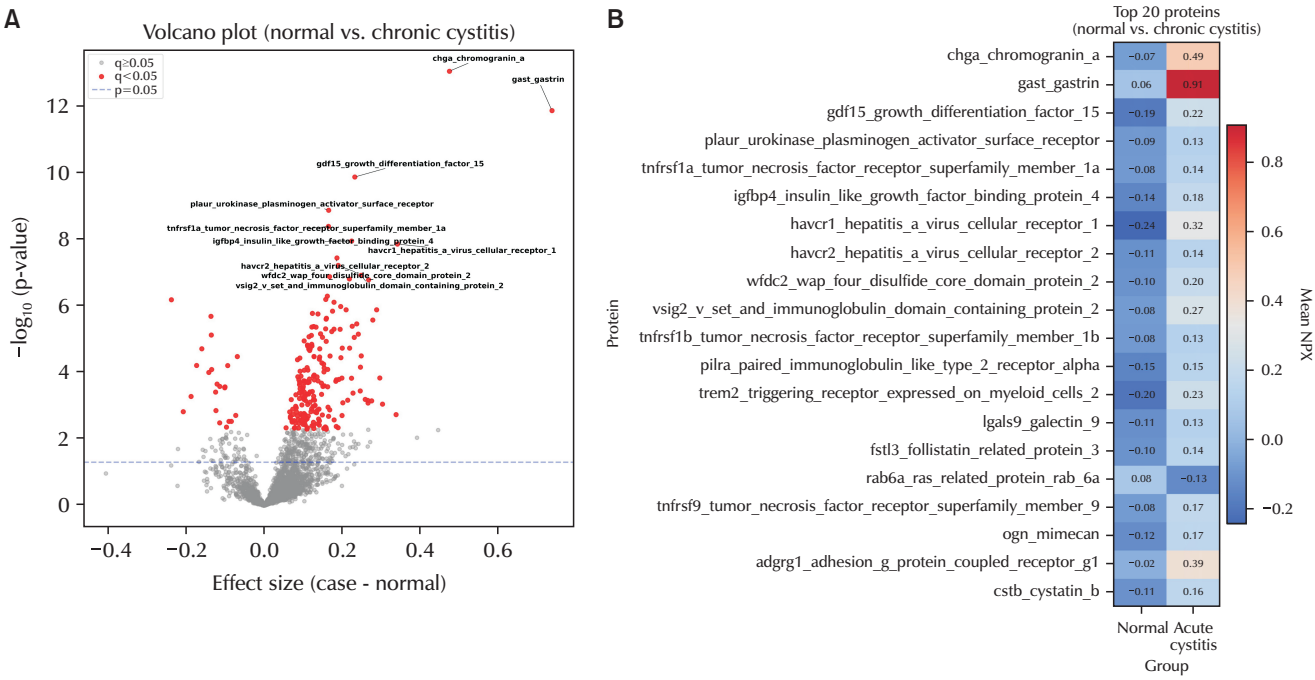

Fig. 3. Differential expression landscape and top protein signatures in chronic cystitis. (A) Volcano plot illustrating the distribution of differential plasma proteins between chronic cystitis and normal individuals. Proteins significantly altered after multiple-testing correction (FDR<0.05) are highlighted in red, whereas nonsignificant proteins appear in grey. Several proteins show strong effect sizes with highly significant p-values, including CHGA, GAST, GDF15, PLAUR, TNFRSF1A, IGFBP4, and HAVCR1/HAVCR2, which are labeled on the plot. These dominant markers indicate substantial molecular perturbations associated with chronic inflammatory remodeling in the urinary tract. (B) Heatmap of the top 20 most significant proteins ranked by p-value, showing mean normalized protein expression (NPX) expression across groups. Chronic cystitis exhibits pronounced upregulation of key inflammatory and epithelial-remodeling proteins, including CHGA, GAST, GDF15, PLAUR, and TNFRSF1A, while certain proteins such as RAB6A and CSTB demonstrate relative downregulation. This expression pattern highlights a distinct proteomic signature of chronic cystitis, characterized by persistent immune activation, epithelial injury signaling, and fibrotic or repair-associated pathways. FDR, false discovery rate; CHGA, chromogranin A; GAST, gastrin; GDF15, growth differentiation factor 15; PLAUR, plasminogen activator, urokinase receptor; TNFRSF1A, tumor necrosis factor receptor superfamily member 1A; IGFBP4, insulin-like growth factor binding protein 4; HAVCR1/HAVCR2, hepatitis A virus cellular receptor 1/2; RAB6A, Ras-related protein Rab-6A; CSTB, cystatin B.

systemic signatures associated with the presence of cystitis. Although CHGA has not been previously investigated in the context of cystitis, prior studies have shown that CHGA is elevated or functionally implicated in several inflammatory and immune-mediated conditions, including inflammatory bowel disease, cardiovascular inflammation, metabolic disorders, and autoimmune diseases [12,17-19], which may explain their elevation across both cystitis phenotypes observed in the present study

In addition to these shared markers, phenotype-specific proteins also distinguished acute from chronic cystitis. Acute cystitis showed a selective increase in CDH2, a calcium-dependent adhesion molecule involved in epithelial remodeling and cell-cell junction dynamics. Although CDH2 has not been directly linked to cystitis in prior studies, its upregulation has been observed in conditions characterized by epithelial turnover, tissue injury, and remodeling, including airway inflammation, renal injury, and gastrointestinal epithelial stress [20-22]. The elevation of CDH2 in acute cystitis therefore may reflect epithelial structural responses detectable in the systemic circulation, although tissue-level confirmation is required.

Although CDH2 has not been previously studied in the context of bladder inflammation or cystitis, its involvement in acute pathological conditions has been described in other disease systems. For example, N-cadherin plays a key role in microenvironmental remodeling

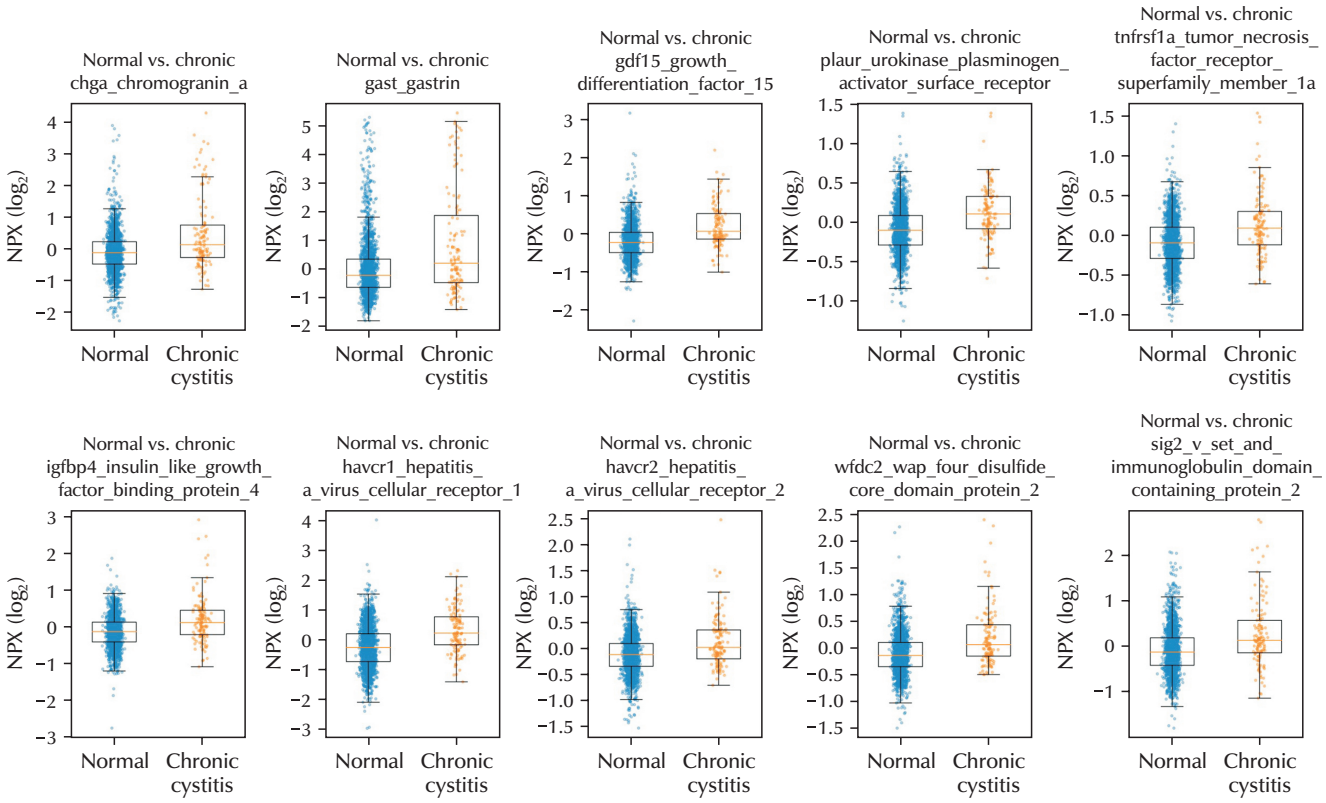

Fig. 4. Box plots of normalized protein expression (NPX) (log_2) levels for the top proteins significantly altered in chronic cystitis. Blue denotes normal controls and orange denotes chronic cystitis. Key markers (*CHGA*, *GAST*, *GDF15*) show strong upregulation, consistent with chronic inflammatory and epithelial stress responses.

[20], cell-cell adhesion [21,22], and stress-responsive signaling in acute leukemia [23,24], suggesting that CDH2 may participate in injury-associated epithelial or stromal responses in acute settings. However, its elevation in acute cystitis observed in our study should be considered hypothesis-generating, and targeted bladder-specific investigations will be required to determine its biological relevance

GDF15 also emerged as one of the most strongly elevated proteins in chronic cystitis, despite the absence of prior studies directly linking this cytokine to bladder inflammation. Although its role in cystitis remains unexplored, GDF15 has been widely described as a systemic stress-response mediator and is known to be upregulated in diverse chronic inflammatory, metabolic, and tissue-injury conditions, including cardiovascular disease [25], chronic kidney disease [26], metabolic syndrome [27-29], and aging-related inflammatory states [30]. Its marked elevation in chronic cystitis may therefore reflect broader systemic or tissue-level stress responses associated with long-standing inflammation. However, given the cross-sectional design and lack of bladder-specific evidence, the interpretation of GDF15 in chronic cystitis should remain cautious and will require dedicated mechanistic and longitudinal studies to determine its clinical significance.

Beyond individual protein-level differences, the PPI network analysis provided additional structural insights into how the differentially abundant proteins may be organized at the systems level in acute versus chronic cystitis. The acute cystitis network displayed a compact, highly interconnected configuration characterized by multiple high-degree nodes and closely clustered interaction modules. This dense architecture suggests that, at the time of sampling, acute cystitis is associated with a more widespread and tightly linked systemic protein

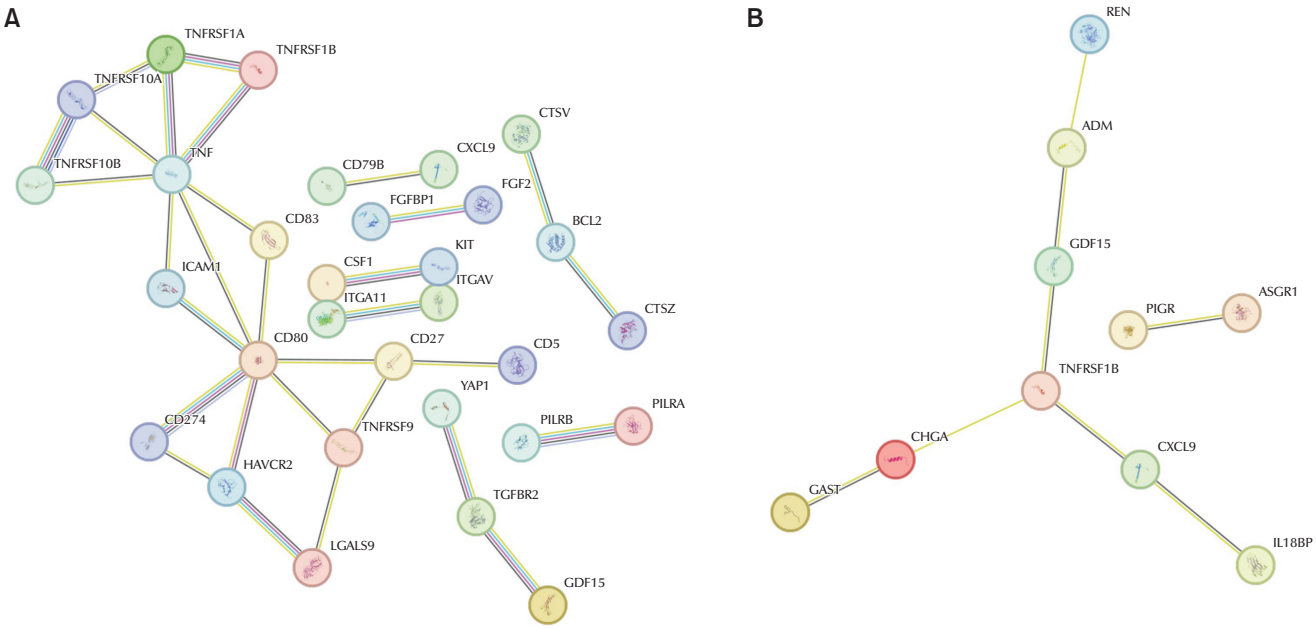

Fig. 5. Protein-protein interaction (PPI) Networks highlighting key biological pathways in acute and chronic cystitis. (A) STRING-derived PPI network of top differentially abundant proteins in acute cystitis. The acute cystitis network demonstrates a highly interconnected module enriched for TNF/TNFRSF family signaling, immune activation, epithelial stress responses, and cell-cell communication nodes (CD80, ICAM1, TNF). Multiple ligand-receptor pairs (e.g., TNFRSF1A/B, CD27–CD70 axis) cluster tightly, suggesting coordinated activation of early inflammatory and epithelial remodeling pathways during acute infection. (B) PPI network of significantly altered proteins in chronic cystitis. Compared with acute cystitis, the chronic network forms a more linear, pathway-focused topology, dominated by CHGA–GAST–GDF15–TNFRSF1B signaling. These proteins represent neuroendocrine stress markers and chronic inflammatory mediators. Additional nodes—including CXCL9, IL18BP, ADM, REN, PILRA, ASGR1—extend the axis toward chronic immune regulation, epithelial injury, and sustained chemokine signaling. Overall, chronic cystitis displays a more streamlined but biologically coherent network reflective of persistent inflammatory remodeling rather than the broad, highly interconnected immune activation seen in acute cystitis. CHGA, chromogranin A; GAST, gastrin; GDF15, growth differentiation factor 15; TNF/TNFRSF, tumor necrosis factor and its receptor superfamily; TNFRSF1B, tumor necrosis factor receptor superfamily member 1B; ICAM1, intercellular adhesion molecule 1; CXCL9, chemokine (C-X-C motif) ligand 9; IL18BP, interleukin-18 binding protein; ADM, adrenomedullin; REN, renin; PILRA, paired immunoglobin-like type 2 receptor alpha; ASGR1, asialoglycoprotein receptor 1.

interaction pattern. However, the clinical or mechanistic significance of this network structure cannot be inferred from the present data.

In contrast, the chronic cystitis network exhibited a more linear and modular topology, with distinct interaction branches centered around proteins such as CHGA, GAST, GDF15, and TNFRSF1B. Compared with the acute network, the chronic network showed fewer total connections and a more segmented organization. These differences may reflect the broader set of elevated proteins observed in chronic cystitis, although the directionality or causal meaning of these network structures remains unknown. Importantly, PPI networks derived from circulating proteins do not capture tissue-specific interactions within the bladder, nor do they distinguish whether elevation of these proteins precedes, accompanies, or follows inflammatory activity. As such, the observed network differences should be interpreted as descriptive representations of systemic protein patterns rather than mechanistic models. Longitudinal sampling, integration with urinary proteomics, and bladder tissue studies will be needed to determine whether these network architectures correspond to biologically meaningful pathways or clinical trajectories in cystitis.

In summary, this population-based proteomic analysis demonstrated that acute and chronic cystitis are associated with distinguishable systemic protein signatures within the UK Biobank cohort. CHGA and GAST were consistently elevated across both phenotypes, suggesting shared neuroendocrine-linked systemic responses

accompanying cystitis, whereas CDH2 and GDF15 showed phenotype-specific differences aligned with acute epithelial remodeling and chronic inflammatory or stress-related pathways, respectively. PPI network analysis further highlighted contrasting interaction architectures between acute and chronic disease, reflecting broader systemic patterns captured in circulating proteomes.

Several limitations should be acknowledged. First, this study was cross-sectional and relied on historical diagnostic records rather than measurements obtained at the time of cystitis onset; therefore, temporal or causal relationships cannot be established. Second, circulating proteomic profiles may not directly reflect bladder-specific molecular processes, and the functional roles of CHGA, GAST, CDH2, and GDF15 in cystitis remain to be validated in tissue-based or mechanistic studies. Third, although age and sex were adjusted for in the regression models, residual confounding by cardiometabolic comorbidities, including diabetes mellitus, hypertension, and dyslipidemia, cannot be excluded, as these variables were not explicitly included as covariates. In addition, unmeasured factors such as medication use or other clinical conditions may have influenced the observed associations. The relatively strict definition of the control group may introduce a healthy reference bias, potentially exaggerating proteomic differences between groups. Finally, the UK Biobank cohort is subject to healthy volunteer bias and underrepresentation of socioeconomically disadvantaged or high-risk populations, which may limit the generalizability of the findings.

CONCLUSIONS

This population-based proteomic analysis demonstrated that acute and chronic cystitis are associated with distinguishable systemic protein signatures in the UK Biobank cohort. CHGA and GAST were consistently elevated across both phenotypes, suggesting shared systemic responses accompanying cystitis, whereas CDH2 and GDF15 showed phenotype-specific differences consistent with acute epithelial remodeling and chronic inflammatory or stress-related processes, respectively. In addition, PPI network analysis revealed contrasting interaction architectures between acute and chronic cystitis, reflecting distinct systemic proteomic patterns captured in circulating plasma. The identified proteins, including CHGA, GAST, CDH2, and GDF15, may serve as candidate circulating biomarkers for differentiating acute and chronic cystitis, although further validation in independent and prospective cohorts is required before clinical application.

NOTES

• **Author Contribution:** Conceptualization: SKK; Data curation: SKK; Formal analysis: SKK; Methodology: SKK; Project administration: SKK; Visualization: SKK; Writing - original draft: CGK, SKK; Writing - review & editing: CGK, SKK.

• **ORCID**
Chang Gu Kang: 0009-0005-2203-1478
Su Kang Kim: 0000-0001-6178-8514

REFERENCES

1. Colgan R, Williams M. Diagnosis and treatment of acute uncomplicated cystitis. Am Fam Physician 2011;84:771-6.
2. Bruyère F, Cariou G, Boiteux JP, Hoznek A, Mignard JP, Escaravage L, et al. [Acute cystitis]. Prog Urol 2008;18 Suppl 1:9-13.
3. Forrest JB, Nickel JC, Moldwin RM. Chronic prostatitis/chronic pelvic pain syndrome and male interstitial cystitis: enigmas and opportunities. Urology 2007;69:60-3.
4. van Ginkel C, Hurst RE, Janssen D. The urothelial barrier in interstitial cystitis/bladder pain syndrome: its form and function, an overview of preclinical models. Curr Opin Urol 2024;34:77-83.
5. Pierce AN, Di Silvestro ER, Eller OC, Wang R, Ryals JM, Christianson JA. Urinary bladder hypersensitivity and dysfunction in female mice following early life and adult stress. Brain Res 2016;1639:58-73.
6. van de Merwe JP. Interstitial cystitis and systemic autoimmune diseases. Nat Clin Pract Urol 2007;4:484-91.

7. Yang Z, Liu Y, Xiang Y, Chen R, Chen L, Wang S, et al. ILC2-derived CGRP triggers acute inflammation and nociceptive responses in bacterial cystitis. Cell Rep 2024;43:114859.
8. Lawrence T. The nuclear factor NF-kappaB pathway in inflammation. Cold Spring Harb Perspect Biol 2009;1:a001651.
9. Mastruzzo C, Greco LR, Nakano K, Nakano A, Palermo F, Pistorio MP, et al. Impact of intranasal budesonide on immune inflammatory responses and epithelial remodeling in chronic upper airway inflammation. J Allergy Clin Immunol 2003;112:37-44.
10. Eldjarn GH, Ferkingstad E, Lund SH, Helgason H, Magnusson OT, Gunnarsdottir K, et al. Large-scale plasma proteomics comparisons through genetics and disease associations. Nature 2023;622:348-58.
11. Lee MA, Burley KL, Hazelwood EL, Moore S, Lewis SJ, Goudswaard LJ. Exploring the role of circulating proteins in multiple myeloma risk: a Mendelian randomization study. Sci Rep 2025;15:3752.
12. Maj M, Hernik K, Tyszkiewicz K, Owe-Larsson M, Sztokfisz-Ignasiak A, Malejczyk J, et al. A complex role of chromogranin A and its peptides in inflammation, autoimmunity, and infections. Front Immunol 2025;16:1567874.
13. De Lorenzo R, Sciorati C, Ramirez GA, Colombo B, Lorè NI, Capobianco A, et al. Chromogranin A plasma levels predict mortality in COVID-19. PLoS One 2022;17:e0267235.
14. Wei J, Wang Y, Yang S, Hao Z, Pan X, Ma A. Plasma chromogranin A levels are associated with acute ischemic stroke with anterior circulation large vessel occlusion. Nutr Metab Cardiovasc Dis 2022;32:195-202.
15. Rehfeld JF, Broedbaek K, Goetze JP, Knigge U, Hilsted LM. True Chromogranin A concentrations in plasma from patients with small intestinal neuroendocrine tumours. Scand J Gastroenterol 2020;55:565-73.
16. Chao C, Hellmich MR. Gastrin, inflammation, and carcinogenesis. Curr Opin Endocrinol Diabetes Obes 2010;17:33-9.
17. Garg R, Agarwal A, Katekar R, Dadge S, Yadav S, Gayen JR. Chromogranin A-derived peptides pancreastatin and catestatin: emerging therapeutic target for diabetes. Amino Acids 2023;55:549-61.
18. Eissa N, Hussein H, Hendy GN, Bernstein CN, Ghia JE. Chromogranin-A and its derived peptides and their pharmacological effects during intestinal inflammation. Biochem Pharmacol 2018;152:315-26.
19. Bandyopadhyay GK, Mahata SK. Chromogranin A regulation of obesity and peripheral insulin sensitivity. Front Endocrinol (Lausanne) 2017;8:20.
20. Bromberg O, Frisch BJ, Weber JM, Porter RL, Civitelli R, Calvi LM. Osteoblastic N-cadherin is not required for microenvironmental support and regulation of hematopoietic stem and progenitor cells. Blood 2012;120:303-13.
21. Sun Z, Parrish AR, Hill MA, Meininger GA. N-cadherin, a vascular smooth muscle cell-cell adhesion molecule: function and signaling for vasomotor control. Microcirculation 2014;21:208-18.
22. Radice GL. N-cadherin-mediated adhesion and signaling from development to disease: lessons from mice. Prog Mol Biol Transl Sci 2013;116:263-89.
23. Parker J, Hockney S, Blaschuk OW, Pal D. Targeting N-cadherin (CDH2) and the malignant bone marrow microenvironment in acute leukaemia. Expert Rev Mol Med 2023;25:e16.
24. Bao BX, An XZ, Li PF, Li YJ, Cui YH, Tang X, et al. [E-cadherin Expression in Children with Acute Leukemia and Its Clinical Significance]. Zhongguo Shi Yan Xue Ye Xue Za Zhi 2019;27:339-47.
25. Folkersen L, Gustafsson S, Wang Q, Hansen DH, Hedman ÅK, Schork A, et al. Genomic and drug target evaluation of 90 cardiovascular proteins in 30,931 individuals. Nat Metab 2020;2:1135-48.
26. Malyszko J, Koc-Zorawska E, Malyszko JS, Glowinska I, Mysliwiec M, Macdougall IC. GDF15 is related to anemia and hepcidin in kidney allograft recipients. Nephron Clin Pract 2013;123:112-7.
27. Keipert S, Ost M. Stress-induced FGF21 and GDF15 in obesity and obesity resistance. Trends Endocrinol Metab 2021;32:904-15.
28. Sabaratnam R, Kristensen JM, Pedersen AJT, Kruse R, Handberg A, Wojtaszewski JFP, et al. Acute exercise increases GDF15 and unfolded protein response/integrated stress response in muscle in type 2 diabetes. J Clin Endocrinol Metab 2024;109:1754-64.
29. Li J, Hu X, Xie Z, Li J, Huang C, Huang Y. Overview of growth differentiation factor 15 (GDF15) in metabolic diseases. Biomed Pharmacother 2024;176:116809.
30. Wan Y, Fu J. GDF15 as a key disease target and biomarker: linking chronic lung diseases and ageing. Mol Cell Biochem 2024;479:453-66.